water

MDPI

Article

Integration of Transcriptomics and Metabolomics for Evaluating Changes in the Liver of Zebrafish Exposed to a Sublethal Dose of Cyantraniliprole

Lijuan Zhao [1,*], Hong Zhang [2], Zhidan Niu [1], Dandan Wei [1], Suyue Yan [1], Jianhua Bai [1], Lei Zhang [1] and Xiaojing Shi [1]

[1] Department of Biology, Xinzhou Normal University, Xinzhou 034000, China
[2] Shanxi Science and Technology Resources and Large-Scale Instruments Open Sharing Center, Taiyuan 030006, China
* Correspondence: zho_001910@126.com; Tel.: +86-188-3512-8920

Abstract: Diamide insecticides are a class of insecticides with high efficiency, a broad spectrum, and environmental and ecological safety. However, their effect on the environment cannot be ignored, especially the chronic environmental effects of sublethal doses. In this study, we evaluated the influence of cyantraniliprole on zebrafish and provided data for evaluating the risk of cyantraniliprole in water. An acute toxicity test was used to obtain LC_{50}, while 1/10 LC_{50} was selected to study the toxicity of the sublethal dose of cyantraniliprole on the transcription and metabolism of zebrafish liver. Our results showed that after exposure to a sublethal dose of cyantraniliprole for 30 days, the expression of various functional genes (*elovl6*, *cpt1ab*, *eci1*, *fabp6*, etc.) was abnormal and the content of various metabolites (*Taurine*, *1-Acyl-sn-glycero-3-phosphocholine*, *phosphatidylserine*, *betaine*, *sarcosine*, etc.) was altered. In addition, transcriptional and metabolic correlation analysis revealed that sublethal doses of cyanobacteria could affect the fatty acid metabolism-related pathways of zebrafish liver (fatty acid elongation, metabolism, and degradation), as well as the PPAR pathway related to fat and the ABC pathway related to drug metabolism and transport. In conclusion, sublethal doses of cyantraniliprole caused abnormal liver metabolism in zebrafish by affecting fatty acid metabolism, up-regulating the PPAR pathway and down-regulating related genes and metabolites in the ABC pathway, which eventually led to liver damage.

Keywords: cyantraniliprole; zebrafish; toxicity; transcriptomics; metabolomics

Citation: Zhao, L.; Zhang, H.; Niu, Z.; Wei, D.; Yan, S.; Bai, J.; Zhang, L.; Shi, X. Integration of Transcriptomics and Metabolomics for Evaluating Changes in the Liver of Zebrafish Exposed to a Sublethal Dose of Cyantraniliprole. *Water* **2023**, *15*, 521. https://doi.org/10.3390/w15030521

Academic Editor: Abasiofiok Mark Ibekwe

Received: 17 November 2022
Revised: 18 January 2023
Accepted: 26 January 2023
Published: 28 January 2023

1. Introduction

Diamide insecticides are a class of insecticide with a special site of action introduced to control planthopper on rice [1], citrus psyllid [2], *Trialeurodes vaporariorum* [3], *Bactrocera dorsalis* [4], *Ostrinia furnacalis* [5], etc. Due to the unique targets of these agents on insects that selective activate the insect ryanodine receptor, diamide insecticides have been applied to more than 200 crops worldwide [6]. At present, commercial pesticides which contain diamide active ingredients include flubendiamide, chlorantraniliprole, cyantraniliprole, cyclaniliprole, and tetrachlorantraniliprole [7]. In China, diamine pesticides are used in large quantities [8–10], which further increases the risk of contamination of aquatic environmental systems [7,11]. In 2018, flubendiamide was banned in China due to its huge toxic effect on the water environment [7]. In addition, there are also reports on the toxicity of cyantraniliprole in non-target organisms. Xu et al. reported that cyantraniliprole could cause DNA damage in the liver cells of tilapia by activating the pathways of DNA damage and repair [5]. More recently, Qiao et al. reported toxicity affecting reproduction, genes, and intestines damage in earthworms after exposure to high doses of cyantraniliprole [12]. Other studies have reported that cyantraniliprole is less toxic to fish, including rainbow trout, sheepshead minnow, bluegill sunfish, and channel catfish; however, cyantraniliprole

has a higher risk of being toxic (both acutely and chronically) to invertebrates [12,13]. The results of chronic toxicity studies on rainbow trout (no observed effect concentration of 10.7 mg/L, 90d) and sheepshead minnow(no observed effect concentration of 9.9 mg/L, 30d) showed that cyantraniliprole is toxic to different species of fish [13]. However, there are no studies on the short-term toxicity of cyantraniliprole in zebrafish, especially at the transcriptional and metabolic levels.

The combination of transcriptome and metabolome was used to analyze biological systems at different levels, as well as different biological organisms [14]. Relevant mechanistic information was obtained through pathway overexpression and enrichment analysis [15]. The combined analysis of transcriptomics and metabolomics is widely used in plant research but is rare in animal studies, especially in aquatic animals. For example, Masami et al. showed that several specific response pathways for *Arabidopsis thaliana* under sulfur deficiency and related stresses could be obtained by combining transcriptome and metabolome analysis [16]. Moreover, Theodore et al. obtained genes and metabolites of rice response to bacterial wilt using a similar method [14].

In order to investigate the changes in the metabolomics and transcriptomics of zebrafish after being exposed to a sublethal dose of cyantraniliprole in water, KEGG and enrichment analysis were used to evaluate the effects of transcriptomics in the liver of zebrafish. UHPLC-Q Exactive HFX, the R program, and the MS2 database were used for metabolite detection, screening, and annotation. Finally, the correlation analysis of differential genes and metabolites was conducted to obtain the action pathway of sublethal doses of cyantraniliprole in zebrafish liver. The data derived from short-term toxicity studies could be used for quantitative risk assessments and the selection of concentrations for chronic studies of cyantraniliprole in water.

2. Materials and Methods

2.1. Reagents and Animals

Cyantraniliprole (Dupont Agrochemical Co., Ltd., Shanghai, China; 94%), Tween-80, and dimethylformamide (DMF) (Solarbio Technology Co., Ltd., Beijing, China) were used.

Adult female zebrafish (three months old, wild-type, AB strain, the China Zebrafish Resource Center, Wuhan, China) were used. The temperature, humidity, and light time of zebrafish rearing were based on previous research reports [17]. After 2 weeks, zebrafish about 2.5 cm long were used for subsequent toxicity tests. Quality parameters included a pH of 7.3, a dissolved oxygen mean of 6.7, and hardness in the range of 80–95 mg L^{-1} (as $CaCO_3$), with all parameters measured weekly. All experiments were performed in accordance with the guidelines of the Animal Care and Use Committee at Xinzhou Teachers University [approval no. SYXK(JIN) 2020-006].

2.2. Determination of LC_{50}

Zebrafish were reared in a 50 L tank for two weeks before toxicity testing and were fed twice daily with solid food (Jiangmen Pengjiang District Dolphin Aquarium Co., Ltd., Jiangmen, China). They were divided into a control group (chlorine-free tap water) and solvent control group (chlorine-free tap water with 0.05% DMF and Tween 80) (10 fish per group) in this period of testing, which was repeated four times. The fresh pesticide solutions were changed every 24 h to ensure exposure levels. The number of deaths was recorded at 24 and 96 h (GB/T [18] 31270.12−2014) and the mortality of zebrafish was calculated. LC_{50} was calculated based on mortality and concentration. There was no feeding during the test.

2.3. Short-Term Exposure Test

A one-month (30-day) short-term toxicity test was performed in accordance with OECD guidelines [19] at 0.35 mg/L (1/10 of LC_{50}, 96 h). The zebrafish were then anesthetized on ice, and their livers were harvested and used for transcriptional and metabolic studies.

2.4. Transcriptome and Metabolic Analysis

The results of preliminary experiments (acute toxicity test and chronic toxicity test) suggested no significant difference from the control to the solvent control, so we chose the solvent control group (CK) as the control in the transcriptome and metabolome analysis.

2.4.1. Transcriptome Analysis

Transcriptional sequencing of the solvent control group and the 0.35 mg/L cyantraniliprole exposure group (S) was performed by Biotree Biotechnologies Co. (Shanghai, China). The extraction, degradation, and contamination monitoring of total RNA and the method of integrity evaluation was based on previous research reports [20,21].

The establishment of a 1 μg RNA sequencing library for each sample, the evaluation of library quality, the analysis of differential expression between control and treatment groups, and the enrichment of differential genes in the KEGG pathway were also based on previous research [21,22].

2.4.2. Metabolic Analysis

The sample (50 mg) was extracted three times via homogenization (35 Hz, 4 min) and ultrasonication (ice bath, 5 min), and the extraction solution was 1000 μL of methanol, acetonitrile, and water (2:2:1, containing isotope-labeled internal standard)). After extraction, the samples were incubated at a low temperature (−40 °C, 1 h) and centrifuged (12,000 rpm, 15 min, 4 °C) to obtain the supernatant. Subsequently, 3 μL of the supernatant was detected using UHPLC-Q Exactive HFX (Vanquish and Orbitrap MS, Thermo Fisher Scientific) with a mobile phase of 25 mmol/L ammonium acetate and sodium hydroxide (pH = 9.75) in water and acetonitrile.

Electrospray ion source parameters were as follows: sheath gas, 30 Arb; auxiliary gas, 25 Arb; capillary, 350 °C; resolution, 60,000 (full MS) and 7500 (MS/MS); collision energy, 10/30/60; the positive source voltage was 3.6 kV and the negative source voltage was −3.2 kV. The raw data were converted into mzXML format and the R program was used for peak detection, extraction, alignment, and integration. The MS2 database (BiotreeDB) was used for metabolite annotation (the cut-off value was 0.3).

2.5. Differential Gene and Metabolite Association Analysis

We used the "spearman" algorithm to analyze the relationship between differential genes and metabolites. The differential genes and metabolites were introduced into the KEGG pathway to find the related pathways that caused the differences. A p value < 0.05 represented statistical significance.

3. Results

3.1. LC_{50} Value

The LC_{50} of zebrafish after exposure to cyantraniliprole at 24 and 96 h was 7.2 mg/L and 3.5 mg/L, respectively, with 95% confidence intervals of 7.1–8.3 mg/L and 3.4–4.0 mg/L, respectively (Table S1). According to test guidelines, cyantraniliprole was considered to cause moderate toxicity.

3.2. Liver Transcription Results

3.2.1. Differential Genes in Groups after Exposure to Cyantraniliprole

A total of 343 significant DEGs (differential genes) were found after exposure to 0.35 mg/L cyantraniliprole (padj < 0.05 and |log2FoldChange| > 0; Figure 1). There were 115 and 228 up-regulated and down-regulated genes, respectively (Table S2).

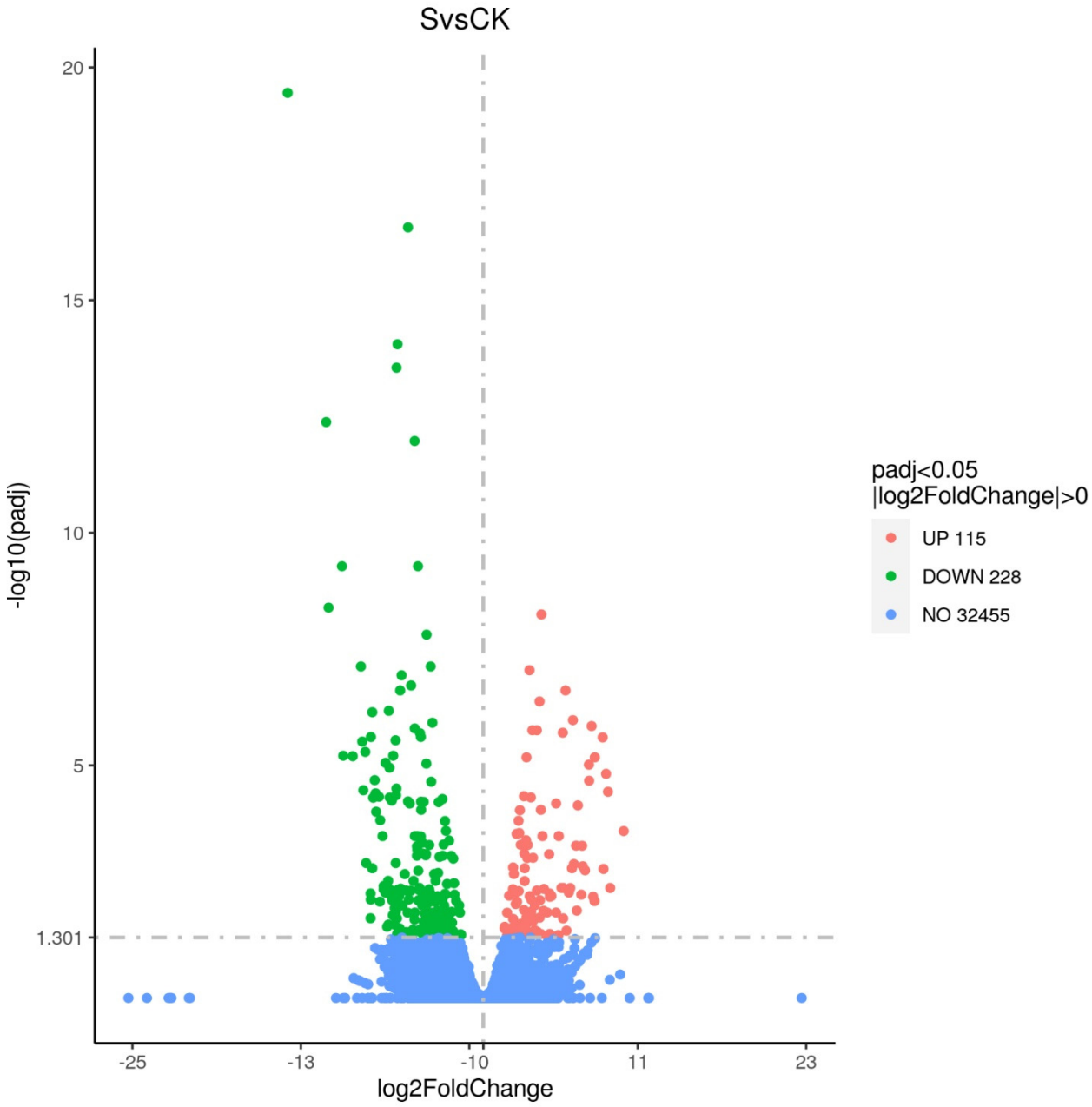

Figure 1. The difference in gene expression between control and treatment groups. Blue dots represent the total number of genes, red dots represent up-regulated genes, and green dots represent down-regulated genes. S—treatment, CK—control.

3.2.2. GO and KEGG Enrichment Results

The clusterProfiler R package was used for GO (Gene Ontology) enrichment of differential genes ($p < 0.05$). Most of the DEGs participated in biological processes (BPs) and molecular function (MF). Eight genes (*fgf19*, *calca*, *cxcl18b*, *fgf9*, *vip*, *ccl19a.2*, *ccl19a.1*, *inhbab*) were down-regulated in MF, including the receptor–ligand activity, receptor regulation, chemokine expression, and the binding of chemokine receptors (Figure 2A). Six genes (*got2a*, *elovl6*, *eci1*, *me1*, *hadhab*, *tph1a*) were up-regulated in BPs, including carboxylic acid catabolism, oxyacid metabolism, organic acid catabolism, fatty acid oxidative catabolism, and small molecule catabolism (Figure 2B).

As shown in Figure 3, there were 20 reliable KEGG (Kyoto Encyclopedia of Genes and Genomes) pathways and differential genes enriched in the pathways. According to padj < 0.05 and $|\log2\ (\text{Fold change})| \geq 1$, four pathways were chosen. Fatty acid degra-

dation and metabolism and the PPAR signaling pathway were enriched in the exposure group, while arginine biosynthesis was down-regulated (Table 1).

3.3. Metabolites Analysis

3.3.1. Differences in Metabolites in Groups Exposed to Cyantraniliprole

There were 764 metabolites detected by UHPLC-MS/MS (quadrupole and Orbitrap), including 556 in the positive ion mode and 208 in the negative ion mode. These metabolites were organic acids, amino acids, lipids, carbohydrates, nucleosides, and alkaloids. The differential metabolites were screened according to $p < 0.05$, VIP > 1. In the positive ion mode, 175 significantly different metabolites were obtained. Among the 71 metabolites that were significantly decreased, 24 metabolites were decreased by more than 0.5 times, while 104 metabolites were significantly increased, among which 13 metabolites increased more than ten-fold compared to the control (Figure 4A, Table 2).

In the negative ion mode, 40 significantly different metabolites were obtained. Thirty-five metabolites were significantly decreased, and three metabolites were reduced by more than 0.5 times vs. the control group. Additionally, four metabolites were significantly increased more than ten-fold compared to controls (Figure 4B, Table 3).

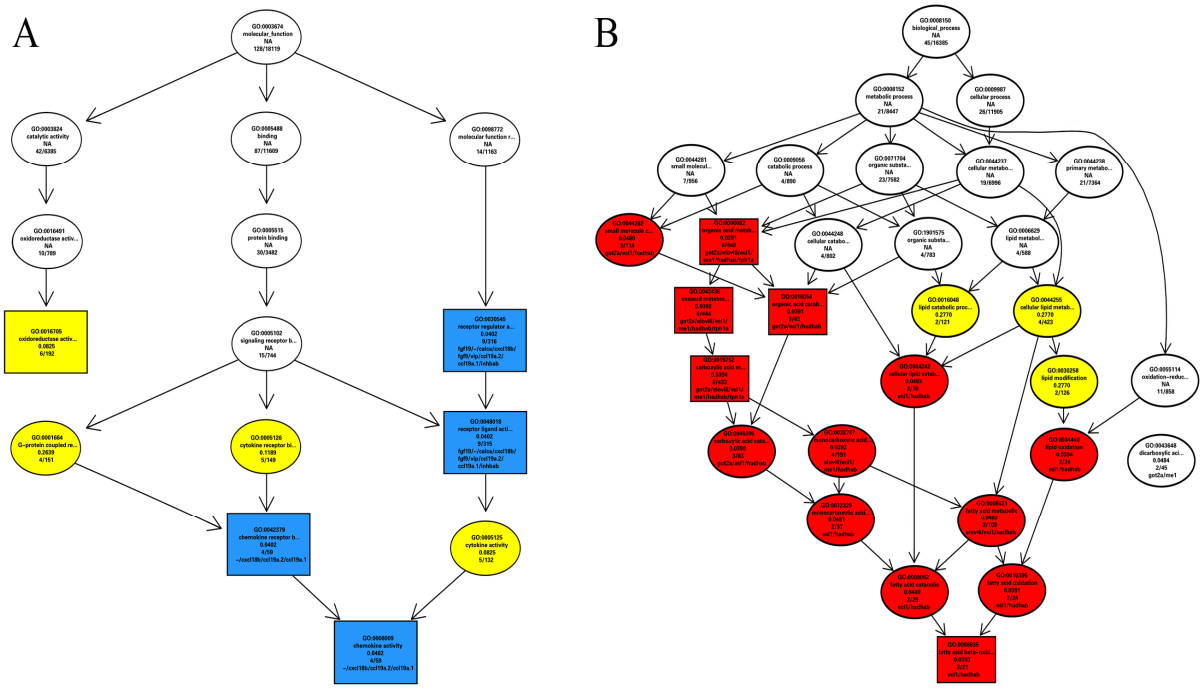

Figure 2. DEGs in BPs (**A**) and MF (**B**). The rectangle represents GO with the enrichment level of TOP5, and the oval is non-Top5. The shade of color expresses the degree of enrichment. In (**A**), blue represents the strongest enrichment, followed by yellow and white representing the weakest enrichment. In (**B**), red represents the strongest enrichment, followed by yellow and white representing the weakest enrichment.

Table 1. Differential genes (padj < 0.05, |log2 (Fold change)| ≥ 1) in the KEGG-related pathways after cyantraniliprole exposure.

KEGGID	Description	padj	GeneID	GeneName	
dre00220	Arginine biosynthesis	0.005	ENSDARG00000069095/ENSDARG00000039269/ENSDARG00000026925/novel.6825	gls2a/arg2/nos2a/-	Down-regulated
dre00071	Fatty acid degradation	0.020	ENSDARG00000062054/ENSDARG00000018002/ENSDARG00000060594/novel.4229	cpt1ab/eci1/hadhab/-	
dre01212	Fatty acid metabolism	0.036	ENSDARG00000062054/ENSDARG00000004402/ENSDARG00000060594/novel.4229	cpt1ab/elovl6/hadhab/-	Up-regulated
dre03320	PPAR signaling pathway	0.041	ENSDARG00000062054/ENSDARG00000044566/ENSDARG00000053215/novel.4229	cpt1ab/fabp6/me1/-	

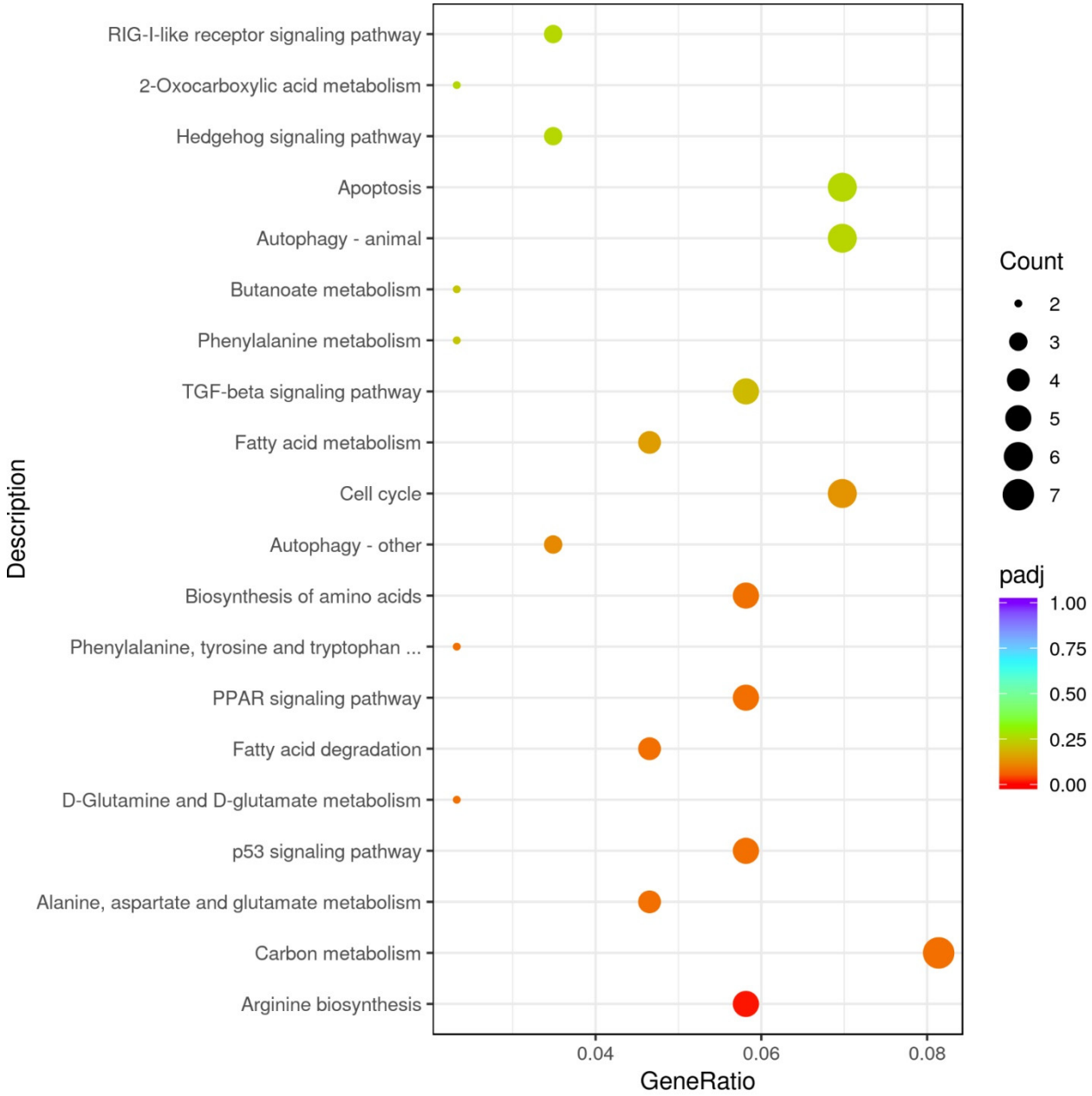

Figure 3. Scatter plot of the 20 most significant KEGG pathways. The size of the dots represents the number of genes annotated to the KEGG pathway, and the color from red to purple represents the significance of the enrichment.

Figure 4. (**A**) Different metabolites under positive ion mode (NEG). (**B**) Different metabolites under negative ion mode (POS). The size of the dot represents the value of LOG_FOLDCHANGE; the smaller the dot, the smaller the corresponding LOG_FOLDCHANGE value. The color of the dot represents the classification of the different metabolite sources in the group and the line represents the correlation coefficient value of the metabolite at the corresponding location.

Table 2. The difference in metabolites in the positive ion mode.

Super Class	MS2 Name	Vip	*p*-Value	Old Change	
Organic acids and derivatives	Betaine	1.1706	0.0290	0.8150	↓
	Creatine	1.2810	0.0016	0.5706	↓
	Creatinine	1.3438	0.0348	0.7076	↓
	Taurine	1.2138	0.0083	0.6915	↓
	N-(2-Methylpropyl) acetamide	1.6595	0.0003	0.5217	↓
	Alanyl-ssparagine	1.4894	0.0019	0.5506	↓
	L-carnitine	1.3082	0.0095	0.7323	↓
	Nervonyl carnitine	1.1347	0.0396	0.5730	↓
	Beta-guanidinopropionic acid	1.5416	0.0003	0.7521	↓
	2-diethylaminoethanol	1.2225	0.0400	0.6536	↓
	Furanone A	1.3682	0.0019	0.6856	↓
	1-isothiocyanato-6-(methylsulfinyl)hexane	1.3442	0.0260	0.6996	↓
	L-acetylcarnitine	1.4341	0.0011	0.6890	↓
	3-hydroxyisovalerylcarnitine	1.3427	0.0150	0.5635	↓
	Leucyl-serine	1.6092	0.0125	11.5661	↑
	3-Chlorotyrosine	1.5789	0.0241	45.8652	↑
	Dihydrocaffeic acid 3-sulfate	1.7584	0.0004	11.6826	↑
Other	PC(18:1(11Z)/14:0)	1.4287	0.0020	0.5528	↓
	PC(16:1(9Z)/P-18:0)	1.3582	0.0074	0.5713	↓
	PS(18:0/22:6(4Z,7Z,10Z,13Z,16Z,19Z))	1.4937	0.0014	0.7067	↓
	Schleicherastatin 5	1.2785	0.0223	0.5590	↓
	Ganodermic acid TQ	1.4614	0.0076	0.5426	↓
Lipids and lipid-like molecules	Linoleamide	1.0443	0.0398	0.7566	↓
	PC(18:1(11Z)/P-16:0)	1.2649	0.0021	0.5305	↓
	PS(18:0/22:6(4Z,7Z,10Z,13Z,16Z,19Z))	1.4937	0.0014	0.7067	↓
	Perilloside B	1.7006	0.0147	142.6186	↑
	2,3-dinor-6-keto-prostaglandin F1 a	1.3067	0.0462	96.1260	↑
	17-phenyl-18,19,20-trinor-prostaglandin E2	1.7325	0.0143	101.8653	↑

Table 2. *Cont.*

Super Class	MS2 Name	Vip	*p*-Value	Old Change	
Nucleosides, nucleotides, and analogues	LysoPC(P-18:1(9Z))	1.5407	0.0172	18.9561	↑
	5′-methylthioadenosine	1.4422	0.0028	0.6312	↓
Phenylpropanoids and polyketides	2′,7-dihydroxy-4′-methoxy-8-prenylflavan	1.7849	0.0105	1565.9867	↑
	1-(4-hydroxy-3,5-dimethoxyphenyl)-7-(4-hydroxy-3-methoxyphenyl)-3,5-heptanediol	1.5020	0.0028	10.0861	↑
	Ethyl trans-p-methoxycinnamate	1.7784	0.0035	213.7491	↑
	Benzyl cinnamate	1.3512	0.0105	0.6595	↓
Organoheterocyclic compounds	Enrofloxacin	1.6447	0.0014	94.0261	↑
	Flumioxazin	1.6558	0.0049	11.2860	↑
Benzenoids	Acetylsalvipisone	1.6715	0.0130	121.9760	↑

Note: "↑" indicates that the metabolite content in the treatment group is higher than that in the control group, and "↓" indicates that the metabolite content in the treatment group is higher than that in the control group.

Table 3. The difference in metabolites in the negative ion mode.

Super Class	Name (MS2)	Vip	*p*-Value	Fold Change	
Lipids and lipid-like molecules	Gamma-linolenic acid	1.1277	0.0282	3.6790	↑
	Androsterone sulfate	1.7047	0.0082	2726.9810	↑
Nucleosides, nucleotides, and analogues	5′-methylthioadenosine	1.7020	0.0427	169.6809	↑
Benzenoids	4-dodecylbenzenesulfonic acid	1.5190	0.0079	9.1142	↑
Organic acids and derivatives	Sarcosine	1.1400	0.0230	0.5179	↓
	L-proline	1.0763	0.0363	0.5444	↓
	Taurine	1.1467	0.0233	0.5079	↓

Note: "↑" indicates that the metabolite content in the treatment group is higher than that in the control group, and "↓" indicates that the metabolite content in the treatment group is higher than that in the control group.

3.3.2. Pathway Analysis of Differential Metabolites

There were eight relevant metabolic pathways in the negative and positive ion modes (lnp values > 0): taurine and hypotaurine, pyrimidine, arginine and proline, glyoxylic acid and dicarboxylic acid metabolism, the tricarboxylic acid cycle (TCA cycle), phenylalanine metabolism, tyrosine and tryptophan biosynthesis, and glycerophospholipid metabolism (Figure 5A,B).

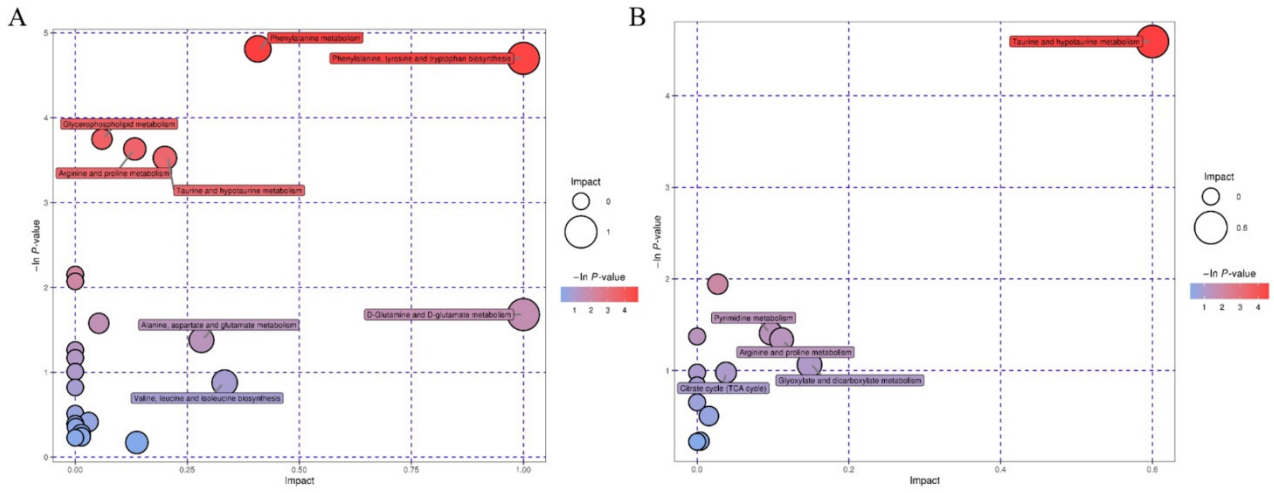

Figure 5. Metabolic pathway profiles of metabolites. The larger the bubble, the greater the influence of the pathway. The red represents a large difference and the white represents a small difference. (**A**) Negative ion mode, (**B**) positive ion mode.

3.4. Correlation Analysis

The correlation between liver tissue differential genes and differential metabolites of zebrafish was analyzed.

Under the negative ion model (Figure 6A), the correlation between seven metabolites and 18 genes was analyzed. *fgf9* showed a significant negative correlation with four metabolites (4-dodecylbenzenesulfonic acid, 5′-methylthioadenosine, androsterone sulfate, and gamma-linolenic acid), *fgf19* and *nos2a* showed a significant negative correlation with three metabolites (4-dodecylbenzenesulfonic acid, 5′-methylthioadenosine, and androsterone sulfate), and *mel* and *captlab* showed a significant positive correlation with the three metabolites.

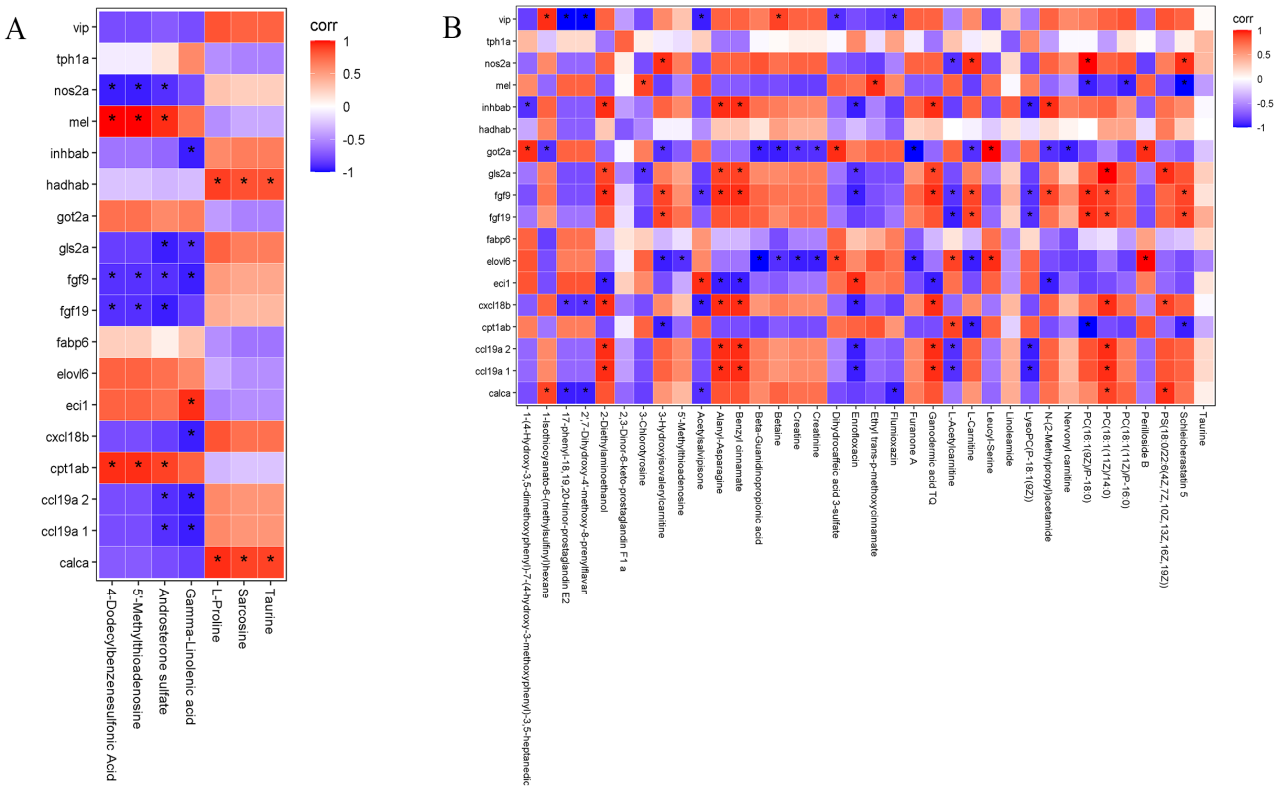

Figure 6. (**A**) Correlation analysis under negative ion mode (NEG). (**B**) Correlation analysis under positive ion mode (POS). Note: red—positive correlation; blue—negative correlation; "*"—$p < 0.05$; dark colors represent strong correlations and light colors represent weak correlations.

gls2a, *ccl19a1*, and *ccl19a2* were significantly negatively correlated with gamma-linolenic acid and androsterone sulfate. *cxcl18b* and *inhbab* were significantly negatively correlated with gamma-linolenic acid, and *inhbab* and *ecil1* showed a significant positive correlation with gamma-linolenic acid. *calca* and *hadbab* showed a significant positive correlation with taurine, sarcosine, and L-proline. *vip*, *tphla*, *got2a*, *fabp6*, and *elovl6* were not correlated with these seven metabolites.

In the positive ion model (Figure 6B), *fabp6, hadhab, and tphla* showed no correlation with 36 metabolites, 2,3 dinor-6-keto-protaglandinF1a, 3-chlorotysine, 5′-methythioadenosine, linoleamide, nervonyl carnitine, and taurine while also showing no correlation with 18 genes. *calca* was positively correlated with three metabolites [1-isothiocyanato-6-(methylsulfinyl) hexane, PC (18:1(11Z)/14:0), and PS (18:0/22:6 (4Z, 7Z, 10Z, 13Z, 16Z, 19Z)] and negatively correlated with four metabolites (acetylsalvipisone, flumioxazin, 2′,7-dihydroxy-4′-methoxy-8-prenylflavan, 17-phenyl-18,19,20-trinor-prostaglandin E2).

ccl19a1 and *ccl19a2* were positively correlated with three metabolites (2-diethylaminoethanol, alanyl-asparagine, benzyl cinnamate and PC (18:1(11Z)/14:0)) and negatively correlated with three metabolites [enrofloxacin, L-acetylcarnitine, lysoPC (P-18:1(9Z)].

exc118b was positively correlated with six metabolites [2-diethylaminethanol, alanyl-asparagine benzyl-cinnamate, ganodermic, PC (18:1(11Z)/14:0), and PS (18:0/22:6 (4Z, 7Z, 10Z, 13Z, 16Z, 19Z)] and negatively correlated with four metabolites (2′,7-dihydroxy -4′-methoxy-8-prenylflavan, 17-phenyl-18,19,20-trinor-prostaglandin E2, acetylsalvipisone, and enrofloxacine).

eci1 had a significant positive correlation with two metabolites (acetylsalvipisone and enrofloxacine) and a negative correlation with five metabolites (2-diethylaminethanol, alanyl-asparagine, benzyl cinnamate, ganodermic acid TQ, and N-(2-Methylpropyl) acetamide).

elov16 was positively correlated with four metabolites (dihydrocaffeic acid 3-sulfate, L-acetylcarnitine, leucyl-serine, and perilloside B) and negatively correlated with eight metabolites (3-hydroxyisovalerylcarnitine, 5′-methylthioadenosine, beta-guanidinopropionic acid, betaine, creatine, creatinine, furanone A, and L-carnitine).

fgf19 was positively correlated with five metabolites (3-hydroxyisovalerylcarnitine, L-carnitine, PC (16:1(9Z)/P-18:0), PC (18:1(11Z)/P-16:0), and schleicherastatin 5) and negatively correlated with two metabolites [L-carnitine and lysoPC (P-18:1(9Z)].

fgf9 was positively correlated with ten metabolites (2-diethylaminoethanol, 3-hydroxyisovalerylcarnitine, alanyl-asparagine, benzyl cinnamate, ganodermic acid TQ, L-carnitine, N-(2-methylpropyl) acetamide, PC(16:1(9Z)/P-18:0), PC (18:1(11Z)/14:0), and schleicherastatin 5) and negatively correlated with four metabolites [acetylsalvipisone, enrofloxacin, L-acetylcarnitine, and lysoPC (P-18:1(9Z)].

gls2a was positively correlated with six metabolites (2-diethylaminoethanol, alanyl-asparagine, benzyl cinnamate, ganodermic acid TQ, PC (18:1(11Z)/14:0), and perilloside B) and negatively correlated with two metabolites (3-chlorotyrosine and enrofloxacin).

got2a was positively correlated with four metabolites (1- (4- hydroxy -3,5-dimethoxyphenyl)-7-(4-hydroxy-3-methoxyphenyl)-3,5-heptanediol, dihydrocaffeic acid 3-sulfate, leucyl-serine, and perilloside B) and negatively correlated with ten metabolites (1-Isothiocyanato-6-(methylsulfinyl) hexane, 3-hydroxyisovalerylcarnitine, beta-guanidinopropionic acid, betaine, creatine, creatinine, furanone A, L-carnitine, N-(2-methylpropyl) acetamide, and nervonyl carnitine).

Inhab was positively correlated with five metabolites (2-diethylaminoethanol, alanyl-asparagine, benzyl cinnamate, ganodermic acid TQ, and N-(2-methylpropyl) acetamide) and negatively correlated with three metabolites (1-(4-hydroxy-3,5 -dimethoxyphenyl)-7-(4-hydroxy-3-methoxyphenyl)-3,5-heptanediol, enrofloxacin, and lysoPC(P-18:1(9Z)).

mel showed a positive correlation with two metabolites (3-chlorotyrosine and ethyl trans-p-methoxycinnamate) and a negative correlation with three metabolites (PC (16:1(9Z)/P-18:0), PC (18:1(11Z)/P-16:0), and schleicherastatin 5).

nos2a showed a correlation with four metabolites (3-hydroxyisovalerylcarnitine, L-carnitine, PC(16:1(9Z)/P-18:0), and schleicherastatin 5) and a negative correlation with L-acetylcarnitine.

vip was positively correlated with two metabolites (1-isothiocyanato-6-(methylsul -finyl) hexane and betaine) and negatively correlated with five metabolites (17-phenyl-18,19,20-trinor-prostaglandinE2, 2′,7-dihydroxy-4′-methoxy-8-prenylflavan, acetylsalvipisone, dihydrocaffeic acid 3-sulfate, and flumioxazin).

These differential genes and metabolites are mainly involved in pathways related to amino acid and fatty acid metabolism (Table 4).

Specifically, two genes (*got2a, nos2a*) and four metabolites (sarcosine, L-proline, creatine, and creatinine) participated in arginine and proline metabolism, one gene (*got2a*) and one metabolite (5′-methylthioadenosine) participated in cysteine and methionine metabolism, two genes (*hadhab*, *tph1a*) participated in tryptophan synthesis, and three metabolites (betaine, creatine, and phosphatidylserine) participated in glycine, serine, and threonine metabolism.

Table 4. Differential genes and metabolites in KEGG-related pathways after cyantraniliprole exposure (padj < 0.05, |log2 (Fold change)| ≥ 1).

KEGG Pathway	Genes and Metabolites
dre01040: biosynthesis of unsaturated fatty acids—Danio rerio (zebrafish) (2)	cpd: C06426 (6Z,9Z,12Z)-octadecatrienoic acid | | dre:317738 elovl6: elongation of very long-chain fatty acids protein 6
dre00062: fatty acid elongation—Danio rerio (zebrafish) (2)	dre:317738 elovl6 | | dre:793834 hadhab: mitochondrial trifunctional protein, alpha subunit
dre01212: fatty acid metabolism—Danio rerio (zebrafish) (3)	dre:317738 elovl6 | | dre:793834 hadhab: mitochondrial trifunctional protein, alpha subunit | | dre:560000 cpt1ab: carnitine O-palmitoyltransferase 1, isoform X2 in liver
dre00071: fatty acid degradation—Danio rerio (zebrafish) (3)	dre:334101 eci1:eci1 enoyl-CoA delta isomerase 1, mitochondrial | | dre:793834 hadhab: mitochondrial trifunctional protein, alpha subunit | | dre:560000 cpt1ab
dre00564: glycerophospholipid metabolism—Danio rerio (zebrafish) (3)	cpd: C04230 1-acyl-sn-glycero-3-phosphocholine | | cpd:C00157 phosphatidylcholine | | cpd:C02737 phosphatidylserine
dre00260: glycine, serine, and threonine metabolism—Danio rerio (zebrafish) (3)	cpd: C00719 betaine | | cpd:C00300 creatine | | cpd:C02737 phosphatidylserine
dre00270: cysteine and methionine metabolism—Danio rerio (zebrafish) (2)	cpd: C00170 5′-methylthioadenosine | | dre:406688 got2a: aspartate aminotransferase 2a
dre00330: arginine and proline metabolism—Danio rerio (zebrafish) (6)	cpd: C00213 sarcosine | | cpd:C00148 L-proline | | dre:406688 got2a: aspartate aminotransferase 2a | | dre:404036 nos2a: nitric oxide synthase 2a, inducible | | cpd:C00300 creatine | | cpd:C00791 creatinine
dre00380: tryptophan metabolism—Danio rerio (zebrafish) (2)	dre:793834 hadhab:hadhab mitochondrial trifunctional protein, alpha subunit | | dre:352943 tph1a: tryptophan 5-hydroxylase 1
dre02010: ABC transporters—Danio rerio (zebrafish) (3)	cpd: C00148 L-proline | | cpd:C00245 taurine | | cpd: C00719 betaine
dre04080: neuroactive ligand–receptor interaction— Danio rerio (zebrafish)(3)	cpd: C00245 taurine | | dre:436744 calca: calcitonin gene-related peptide 2 precursor | | dre:795653 vip: VIP peptides
dre01200: carbon metabolism—Danio rerio (zebrafish) (2)	dre:406688 got2a:got2a aspartate aminotransferase 2a | | dre:793834 hadhab: mitochondrial trifunctional protein, alpha subunit
dre03320: PPAR signaling pathway—Danio rerio (zebrafish) (2)	dre:415166 fabp6:fabp6 gastrotropin | | dre:560000 cpt1ab

One gene (*elovl6*) and one metabolite ((6Z,9Z,12Z)-octadecatrienoic acid) participated in unsaturated fatty acid biosynthesis, two genes (*elovl6*, *hadhab*) participated in fatty acid elongation, three genes (*elovl6*, *hadhab*, *and cpt1ab*) participated in fatty acid metabolism, another three genes (*eci1*, *hadhab*, *and cpt1ab*) participated in fatty acid degradation, two genes (*fabp6*, *cpt1ab*) participated in the PPAR signaling pathway, and three metabolites (L-proline, taurine, and betaine) participated in ABC transporters.

4. Discussion

The LC_{50} of cyantraniliprole was 3.5 mg/L(96 h), which indicates moderate toxicity to zebrafish according to the acute toxicity test. This result is inconsistent with that of tilapia (slight toxicity) [5], which may be caused by the different size of the fish.

In the present study, we studied the changes in transcriptome and metabolome in the liver of zebrafish exposed to sublethal doses of cyantraniliprole. A previous study reported that cyantraniliprole could induce DNA damage in the liver cells of tilapia [5]. We also found that cyantraniliprole induced differential expression of multiple genes and metabolites in the liver of zebrafish. The correlation of differential genes and metabolites suggested that *gls2a*, *inhab*, *cxcl18b*, *elovl6*, *fgf9*, and *got2a* were associated with more than eight metabolites and involved in multiple metabolic pathways.

The conversion of glutamate and glutamine involves three key enzymes, of which glutamine synthase catalyzes glutamine production from glutamate, while GLS and GLS2 catalyze the breakdown of glutamine to glutamate. In the present study, one paralog of glutaminase2 (*Gls2a*) was identified in the liver of zebrafish, which is consistent with the report of specific *gls2a* expression in the liver of 120 hpf wild-type zebrafish larvae [23].

Furthermore, the obtained result indicated that *gls2a* was negatively correlated with 3-chlorotyrosine in phenylalanine metabolism downstream of glutamine and positively correlated with alanyl-asparagine.

Elovl6 participates in insulin resistance, obesity, and adipogenesis [24]. Furthermore, a previous study showed that *Elovl6* expression is up-regulated in human hepatoma cells and is associated with nonalcoholic steatohepatitis-induced hepatocarcinogenesis [25]. In our study, *Elovl6* was up-regulated after exposure to the sublethal dose of cyantraniliprole, indicating that long-term exposure can lead to liver damage. In addition, the up-regulation of *Elovl6* led to a decrease in the content of creatine and creatinine in the amino acid metabolism pathway.

The *inhab* gene encodes the βA subunit of activin or inhibin, which is involved in the reproductive and developmental processes of the organism [26]. Some studies have detected that the up-regulated expression of *inhab* is closely related to various human cancers, such as esophageal cancer, colon cancer, and lung cancer, and may participate in the occurrence and development of tumors [27–31]. However, in this study, we found that a sublethal dose of cyantraniliprole had no significant effect on *inhab*, which suggests that this gene may not be the main target for inducing liver damage.

Increased NH_4^+ concentration affected mRNA expression, causing an increase in *GOT1* and *GOT2a*, which is indicative of an increase in the transamination process of aspartate aminotransferase that affects the tricarboxylic acid cycle [32]. In the present study, we observed up-regulated expression of *got2a* in zebrafish liver after exposure to a sublethal dose of cyantraniliprole. Our data indicated that *got2a* is also involved in various amino acid metabolisms, such as arginine, proline, cysteine, and methionine metabolism, among others. Furthermore, these results indicate that sublethal doses of cyantraniliprole induce abnormalities in the tricarboxylic acid cycle and the metabolism of various amino acids.

KEGG pathway enrichment analysis indicated alterations in the metabolism of fatty acids, which involved unsaturated fatty acid biosynthesis, the elongation, metabolism, and degradation of fatty acids, glycerophospholipid metabolism, and PPAR pathways. The PPAR pathway is associated with various liver diseases [33]. Previous studies have shown that the expression or inactivation of PPAR is related to metabolic liver diseases, virus-induced liver diseases, hepatocellular adenomas, and liver cancers [33]. PPAR mainly participates in the regulation of cholesterol and bile homeostasis, inflammation, hepatocyte differentiation, proliferation and regeneration, and other physiological functions at the transcriptional level and is a ligand-activated nuclear receptor [33]. In the present study, the *fabp6* gene was up-regulated in the PPAR pathway, which is a key gene for unsaturated fatty acids in the liver. γ linolenic acid in unsaturated fatty acids was also significantly up-regulated. At the same time, *Capt1b*, a related gene that regulates fatty acid oxidation, was also up-regulated, indicating that sublethal doses of cyantraniliprole affected zebrafish liver transcription and metabolism, resulting in liver damage.

In addition, down-regulation of the ABC transporter pathway and the abnormal metabolism of various amino acids were also seen after exposure to cyantraniliprole. It is well known that the liver is the main organ of drug metabolism and excretion, among which the ABC transporter family is mainly an efflux transporter [34]. Relevant studies have suggested that changes in the expression of ABC transporter mRNA and protein are related to various liver diseases, such as alcoholic steatohepatitis, cirrhosis, and cancer of the liver. [35–39]. The metabolites proline, taurine, and betaine, which are associated with ABC transporters, were all significantly elevated in this study. Relevant research has suggested that taurine and betaine can protect the liver. Taurine combines with bile acids and participates in the excretion of bile, which can alleviate related diseases caused by cholestasis [40]. Betaine can reduce enterogenic endotoxemia, hyperhomocysteinemia, hepatic endoplasmic reticulum stress response [41], and the synthesis and release of pro-inflammatory factors by regulating the polarization process of macrophages [42]. Moreover, it can inhibit the liver's inflammatory response, delay the process of liver cirrhosis, and exert an important role in protecting the liver [43].

To sum up, transcriptomics and metabolomics showed that sublethal doses of cyantraniliprole affect zebrafish liver fatty acid metabolism and ABC transporters, resulting in abnormal fatty acid transcription and metabolism in the liver while stimulating the production of taurine. During this process, increased levels of substances such as acid and betaine are produced to protect the liver; however, the site of action of the specific pathway was not investigated in this study. A more detailed mechanism of action remains to be studied.

Supplementary Materials: The following supporting information can be downloaded at: https://www.mdpi.com/article/10.3390/w15030521/s1, Table S1: The LC_{50} of zebrafish after exposure to cyantraniliprole at 24 and 96 hours; Table S2: The up-regulated and down-regulated genes after exposure to cyantraniliprole.

Author Contributions: L.Z. (Lijuan Zhao) wrote the paper. H.Z. and Z.N. conducted acute toxicity tests of the zebrafish. D.W. and S.Y. performed transcriptomic analysis of the zebrafish. J.B. and L.Z. (Lei Zhang) performed metabolomics analysis of the zebrafish. X.S. was responsible for quality control for all tests. All authors have read and agreed to the published version of the manuscript.

Funding: This research was supported by grants from the Key Research and Development Projects of Shanxi Province (Nos. 201903D321005, and 201903D311001), the Scholar Support Plan of Shanxi, initial doctorate funding of the Xinzhou Teacher University (No. 00000412), the Scientific and Technological Innovation Programs of Higher Education Institutions in Shanxi (Nos. 2019L0832 and 2020L0547), and the Basic Research Program of Shanxi Province (No. 202203021212178).

Data Availability Statement: All data generated or analyzed during this study are included in this published article.

Conflicts of Interest: The authors declare no conflict of interest.

References

1. Wei, W.; Lijuan, X.; Yanping, Z.; Chenyan, L.; Wenwen, P.; Ziming, W.; Xugen, S. Screening of effective pesticides for control of important diseases and insect pests of double cropping rice in jiang xi. *Plant Prot.* **2022**, *48*, 312–319.
2. Tiwari, S.; Stelinski, L.L. Effects of cyantraniliprole, a novel anthranilic diamide insecticide, against Asian citrus psyllid under laboratory and field conditions. *Pest Manag. Sci.* **2013**, *69*, 1066–1072. [CrossRef] [PubMed]
3. Moreno, I.; Belando, A.; Grávalos, C.; Bielza, P. Baseline susceptibility of Mediterranean strains of *Trialeurodes vaporariorum* (Westwood) to cyantraniliprole. *Pest Manag. Sci.* **2018**, *74*, 1552–1557. [CrossRef] [PubMed]
4. Zhang, R.; Jang, E.B.; He, S.; Chen, J. Lethal and sublethal effects of cyantraniliprole on *Bactrocera dorsalis* (Hendel) (Diptera: Tephritidae). *Pest Manag. Sci.* **2015**, *71*, 250–256. [CrossRef] [PubMed]
5. Xu, C.; Ding, J.; Zhao, Y.; Luo, J.; Mu, W.; Zhang, Z. Cyantraniliprole at Sublethal Dosages Negatively Affects the Development, Reproduction, and Nutrient Utilization of *Ostrinia furnacalis* (Lepidoptera: Crambidae). *J. Econ. Entomol.* **2017**, *110*, 230–238. [CrossRef]
6. Ares, A.M.; Valverde, S.; Bernal, J.L.; Toribio, L.; Nozal, M.J.; Bernal, J. Determination of flubendiamide in honey at trace levels by using solid phase extraction and liquid chromatography coupled to quadrupole time-of-flight mass spectrometry. *Food Chem.* **2017**, *232*, 169–176. [CrossRef] [PubMed]
7. Ma, W.; Li, J.; Li, X.; Liu, H. Enrichment of diamide insecticides from environmental water samples using metal-organic frameworks as adsorbents for determination by liquid chromatography tandem mass spectrometry. *J. Hazard. Mater.* **2022**, *422*, 126839. [CrossRef]
8. Wang, M.; Wang, K.; Liu, F.; Mu, W. Comparison of the bioactivity of cyantraniliprole and chlorantraniliprole against three important lepidopterous pests. *Acta Phytophylacica Sin.* **2014**, *41*, 360–366.
9. Caballero, R.; Schuster, D.J.; Smith, H.A.; Mangandi, J.; Portillo, H.E. A systemic bioassay to determine susceptibility of the pepper weevil, *Anthonomus eugenii* Cano (Coleoptera: Curculionidae) to cyantraniliprole and thiamethoxam. *Crop Prot.* **2015**, *72*, 16–21. [CrossRef]
10. Grout, T.G.; Stephen, P.R.; Rison, J.-L. Cyantraniliprole can replace malathion in baits for *Ceratitis capitata* (Diptera: Tephritidae). *Crop Prot.* **2018**, *112*, 304–312. [CrossRef]
11. Jiang, J.; Wang, Y.; Mu, W.; Zhang, Z. Sublethal effects of anthranilic diamide insecticides on the demographic fitness and consumption rates of the *Coccinella septempunctata* (Coleoptera: Coccinellidae) fed on *Aphis craccivora*. *Environ. Sci. Pollut. Res. Int.* **2020**, *27*, 4178–4189. [CrossRef] [PubMed]
12. Qiao, Z.; Yao, X.; Liu, X.; Zhang, J.; Du, Q.; Zhang, F.; Li, X.; Jiang, X. Transcriptomics and enzymology combined five gene expressions to reveal the responses of earthworms (*Eisenia fetida*) to the long-term exposure of cyantraniliprole in soil. *Ecotoxicol. Environ. Saf.* **2021**, *209*, 111824. [CrossRef] [PubMed]

13. European Food Safety Authority. Conclusion on the peer review of the pesticide risk assessment of the active substance cyantraniliprole. *EFSA J.* **2014**, *12*, 3814.
14. Sana, T.R.; Fischer, S.; Wohlgemuth, G.; Katrekar, A.; Jung, K.H.; Ronald, P.C.; Fiehn, O. Metabolomic and transcriptomic analysis of the rice response to the bacterial blight pathogen *Xanthomonas oryzae* pv. *oryzae*. *Metab. Off. J. Metab. Soc.* **2010**, *6*, 451–465. [CrossRef] [PubMed]
15. Kamburov, A.; Cavill, R.; Ebbels, T.M.; Herwig, R.; Keun, H.C. Integrated pathway-level analysis of transcriptomics and metabolomics data with IMPaLA. *Bioinformatics* **2011**, *27*, 2917–2918. [CrossRef]
16. Hirai, M.Y.; Yano, M.; Goodenowe, D.B.; Kanaya, S.; Kimura, T.; Awazuhara, M.; Arita, M.; Fujiwara, T.; Saito, K. Integration of transcriptomics and metabolomics for understanding of global responses to nutritional stresses in *Arabidopsis thaliana*. *Proc. Natl. Acad. Sci. USA* **2004**, *101*, 10205–10210. [CrossRef] [PubMed]
17. Zhang, H.; Zhao, L. Influence of sublethal doses of acetamiprid and halosulfuron-methyl on metabolites of zebra fish (*Brachydanio rerio*). *Aquat. Toxicol.* **2017**, *191*, 85–94. [CrossRef]
18. *GB/T 31270.12-2014*; Test No. 31270. 12: Test Guidelines on Environmental Safety Assessment for Chemical Pesticides—Part 12: Fish Acute Toxicity Test. General Administration of Quality Supervision, Inspection and Quarantine of the People's Republic of China: Beijing, China; Standardization Administration of China: Beijing, China, 2014. (In Chinese)
19. Organization for Economic Co-Operation and Development (OECD). *Test No. 229: Fish Short Term Reproduction Assay*; Organization for Economic Co-Operation and Development (OECD): Paris, France, 2012.
20. Li, T.; Qin, S.; Sun, X.; Zhang, K.-X.; Ding, X.-Y.; Wang, X.-Y.; Li, M.-W. Transcriptome analysis reveals distinct innate immunity and ribosomal response at early stage of AcMNPV infection in haemocyte of silkworm resistant and susceptible strains. *J. Asia Pac. Entomol.* **2022**, *25*, 101938. [CrossRef]
21. Chen, H.; Feng, W.; Chen, K.; Qiu, X.; Xu, H.; Mao, G.; Zhao, T.; Ding, Y.; Wu, X. Transcriptomic analysis reveals potential mechanisms of toxicity in acombined exposure to dibutyl phthalate and diisobutyl phthalate in zebrafish (*Danio rerio*) ovary. *Aquat. Toxicol.* **2019**, *216*, 105290. [CrossRef]
22. Li, Y.; Li, X.; Xiong, L.; Tang, J.; Li, L. Comparison of phenotypes and transcriptomes of mouse skin-derived precursors and dermal mesenchymal stem cells. *Differentiation* **2018**, *102*, 30–39. [CrossRef]
23. Weger, M.; Weger, B.D.; Görling, B.; Poschet, G.; Yildiz, M.; Hell, R.; Luy, B.; Akcay, T.; Güran, T.; Dickmeis, T.; et al. Glucocorticoid deficiency causes transcriptional and post-transcriptional reprogramming of glutamine metabolism. *EBioMedicine* **2018**, *36*, 376–389. [CrossRef] [PubMed]
24. Feng, Y.H.; Chen, W.Y.; Kuo, Y.H.; Tung, C.L.; Tsao, C.J.; Shiau, A.L.; Wu, C.L. Elovl6 is a poor prognostic predictor in breast cancer. *Oncol. Lett.* **2016**, *12*, 207–212. [CrossRef] [PubMed]
25. Muir, K.; Hazim, A.; He, Y.; Peyressatre, M.; Kim, D.Y.; Song, X.; Beretta, L. Proteomic and lipidomic signatures of lipid metabolism in NASH-associated hepatocellular carcinoma. *Cancer Res.* **2013**, *73*, 4722–4731. [CrossRef] [PubMed]
26. Brown, C.W.; Houston-Hawkins, D.E.; Woodruff, T.K.; Matzuk, M.M. Insertion of *Inhbb* into the *Inhba* locus rescues the *Inhba*-null phenotype and reveals new activin functions. *Nat. Genet.* **2000**, *25*, 453–457. [CrossRef] [PubMed]
27. Seder, C.W.; Hartojo, W.; Lin, L.; Silvers, A.L.; Wang, Z.; Thomas, D.G.; Giordano, T.J.; Chen, G.; Chang, A.C.; Orringer, M.B.; et al. INHBA overexpression promotes cell proliferation and may be epigenetically regulated in esophageal adenocarcinoma. *J. Thorac. Oncol.* **2009**, *4*, 455–462. [CrossRef] [PubMed]
28. Lyu, S.; Jiang, C.; Xu, R.; Huang, Y.; Yan, S. INHBA upregulation correlates with poorer prognosis in patients with esophageal squamous cell carcinoma. *Cancer Manag. Res.* **2018**, *10*, 1585–1596. [CrossRef]
29. Okano, M.; Yamamoto, H.; Ohkuma, H.; Kano, Y.; Kim, H.; Nishikawa, S.; Konno, M.; Kawamoto, K.; Haraguchi, N.; Takemasa, I.; et al. Significance of INHBA expression in human colorectal cancer. *Oncol. Rep.* **2013**, *30*, 2903–2908. [CrossRef]
30. Grigoroiu, M.; Tagett, R.; Draghici, S.; Dima, S.; Nastase, A.; Florea, R.; Sorop, A.; Ilie, V.; Bacalbasa, N.; Tica, V.; et al. Gene-expression Profiling in Non-small Cell Lung Cancer with Invasion of Mediastinal Lymph Nodes for Prognosis Evaluation. *Cancer Genom. Proteom.* **2015**, *12*, 231–242.
31. Liang, Z.; Bin, W.; Dongfeng, C. Bioinformatics analysis of expression and clinical significance of INHBA gene in gastric cancer. *Chin. J. Gastroenterol. Hepatol.* **2021**, *30*, 133–138.
32. Probst, J.; Kölker, S.; Okun, J.G.; Kumar, A.; Gursky, E.; Posset, R.; Hoffmann, G.F.; Peravali, R.; Zielonka, M. Chronic hyperammonemia causes a hypoglutamatergic and hyperGABAergic metabolic state associated with neurobehavioral abnormalities in zebrafish larvae. *Exp. Neurol.* **2020**, *331*, 113330. [CrossRef]
33. Peyrou, M.; Ramadori, P.; Bourgoin, L.; Foti, M. PPARs in Liver Diseases and Cancer: Epigenetic Regulation by MicroRNAs. *PPAR Res.* **2012**, *2012*, 757803. [CrossRef] [PubMed]
34. Yujie, Y.; Lei, L.; Miao, X.; Xuehua, J. Significance of regulating liver transporters in the prevention and treatment of liver diseases. *W. China J. Pharm. Sci.* **2020**, *35*, 316–324.
35. Canet, M.J.; Hardwick, R.N.; Lake, A.D.; Dzierlenga, A.L.; Clarke, J.D.; Cherrington, N.J. Modeling human nonalcoholic steatohepatitis-associated changes in drug transporter expression using experimental rodent models. *Drug Metab. Dispos. Biol. Fate Chem.* **2014**, *42*, 586–595. [CrossRef] [PubMed]
36. Ogasawara, K.; Terada, T.; Katsura, T.; Hatano, E.; Ikai, I.; Yamaoka, Y.; Inui, K. Hepatitis C virus-related cirrhosis is a major determinant of the expression levels of hepatic drug transporters. *Drug Metab. Pharmacokinet.* **2010**, *25*, 190–199. [CrossRef]

37. Raafat, N.; Abdel Aal, S.M.; Abdo, F.K.; El Ghonaimy, N.M. Mesenchymal stem cells: In vivo therapeutic application ameliorates carbon tetrachloride induced liver fibrosis in rats. *Int. J. Biochem. Cell Biol.* **2015**, *68*, 109–118. [CrossRef]
38. Geier, A.; Kim, S.K.; Gerloff, T.; Dietrich, C.G.; Lammert, F.; Karpen, S.J.; Stieger, B.; Meier, P.J.; Matern, S.; Gartung, C. Hepatobiliary organic anion transporters are differentially regulated in acute toxic liver injury induced by carbon tetrachloride. *J. Hepatol.* **2002**, *37*, 198–205. [CrossRef] [PubMed]
39. Januchowski, R.; Zawierucha, P.; Andrzejewska, M.; Ruciński, M.; Zabel, M. Microarray-based detection and expression analysis of ABC and SLC transporters in drug-resistant ovarian cancer cell lines. *Biomed. Pharmacotherapy.* **2013**, *67*, 240–245. [CrossRef]
40. Lijuan, Z.; Fang, H.; Zhihua, H. Expression of Na^+-taurocholate co-transporting peptide in liver of rats with acute intrahepatic cholestatic hepatic injury. *J. Clin. Pediatr.* **2009**, *27*, 922–925.
41. Jingquan, J.; Huiying, Z.; Jiantao, J.; Lili, Z.; Yuxia, C.; Limin, W.; Xiaoxia, T.; Ming, F.; Zhongfu, Z.; Dewu, H. Role of 78 kD glucose-regulated protein in the development of liver cirrhosis promoted by intestinal endotoxemia in rats. *Chin. J. Pathophysiol.* **2010**, *26*, 2447–2452.
42. Xiaoxia, T.; Huiying, Z.; Yunxia, C.; Xutong, L.; Limin, W.; Li, M.; Lina, L.; Zhongyang, Z.; Dewu, H. Effects of macrophage polarization during development of liver cirrhosis in rats. *Chin. J. Pathophysiol.* **2016**, *32*, 880–885.
43. Ohashi, W.; Hattori, K.; Hattori, Y. Control of Macrophage Dynamics as a Potential Therapeutic Approach for Clinical Disorders Involving Chronic Inflammation. *J. Pharmacol. Exp. Ther.* **2015**, *354*, 240–250. [CrossRef] [PubMed]